LETTER

Dragon-king extreme events as precursors for catastrophic transition

To cite this article: D. Premraj *et al* 2021 *EPL* **134** 34006

A Letters Journal Exploring the Frontiers of Physics

May 2021

EPL, **134** (2021) 34006
doi: 10.1209/0295-5075/134/34006

www.epljournal.org

Dragon-king extreme events as precursors for catastrophic transition

D. Premraj[1(a)], Kumarasamy Suresh[2], Samadhan A. Pawar[1], Lipika Kabiraj[3], Awadhesh Prasad[2] and R. I. Sujith[1]

[1] *Department of Aerospace Engineering, Indian Institute of Technology Madras - Chennai 600036, India*
[2] *Department of Physics and Astrophysics, University of Delhi - Delhi 110007, India*
[3] *Department of Mechanical Engineering, Indian Institute of Technology Ropar - Punjab 140001, India*

received 23 February 2021; accepted in final form 15 April 2021
published online 15 July 2021

Abstract – Unexpected catastrophic transitions are often observed in complex systems. However, the prediction of such transitions is difficult in practice. Here, we find a special kind of extreme events with a dragon-king probability distribution that occur just prior to a catastrophic transition and, hence, can serve as its precursor. To illustrate the application of dragon kings as a precursor, we consider a practical experimental thermo-fluid system and a theoretical model of coupled logistic maps with quasi-periodic forcing, both systems displaying a catastrophic transition.

Introduction. – Many natural, societal and engineering systems show extreme or rare events that lead to disasters. These events include floods, cyclones, droughts, pandemics, power outages, material ruptures, explosions, chemical contamination, stock market crashes and transmissible diseases (*e.g.*, AIDS, and influenza) [1–4]. The probability of occurrence of such extreme events is low; however, the losses incurred by their presence are enormous. Furthermore, the prediction of the onset of such events is still not mastered. Nevertheless, recent studies systematically explored the occurrence of such events in dynamical systems [5–10]. Extreme events occur in both linear and nonlinear dynamical systems [5–12]. Such events are observed in many physical systems including oceanic rogue waves [13], optical fibers [14], superfluid helium [15], plasmas [16], lasers [17–20], neuronal models [21], etc.

The probability distribution of events in a system follows a power law, where the extreme events appear in the tail of the distribution [1,22,23]. This power-law distribution suggests that the underlying mechanism of all events remains the same across the whole spectrum. This means both regular and extreme events belong to the same population (or the same distribution), reflecting the same underlying mechanism. It has been commonly reported that extreme events are unpredictable because we cannot anticipate the final size (magnitude) of a future event [22,23]. The identification of the origin of extreme events has been a focus of many recent studies [21,24,25].

Sornette [22] examined whether the extreme events in the distribution of events have the same mechanism as the rest of the events (nonextreme events) or they have a different mechanism. From many investigations [22,23], Sornette found that a class of the extreme events deviate from the power law and he termed them "dragon kings". He also showed that dragon kings appear as a result of amplifying mechanisms that are not necessarily active for the rest of the population in the distribution [22]. As a result, the tail of the distribution shows a hump-like behavior for dragon-king extreme events, whereas an extreme event without dragon kings obey a power law. Since dragon kings are rare, losses resulting from these events are more harmful than other events. Dragon kings have been reported in nonlinear electronic circuits [26], bursting neurons [27], distribution of city sizes, distribution of financial draw-downs, and distribution of earthquake energies [22,23,28].

In this paper, we investigate the occurrence of dragon-king extreme events in experiments performed on a thermoacoustic system a ducted laminar premixed flame combustor. Such a system is prone to the occurrence of thermoacoustic instabilities, caused by the positive feedback between the heat release rate fluctuations in the flame and the acoustic field in the confinement, resulting in large-amplitude acoustic oscillations [29]. These instabilities manifest various dynamical behaviors such as limit

(a) E-mail: premraj2891@gmail.com (corresponding author)

cycle, period-2, quasi-periodicity, intermittency, chaos and strange nonchaos [30–33]. The presence of thermoacoustic instability in a combustion system can lead to structural damage of the system components and overwhelm the thermal protection systems; hence, their occurrence is undesirable [29]. Similar to thermoacoustic instability, flame blowout is another catastrophic phenomenon observed in such a system [34]. Prior to flame blowout, Kabiraj and Sujith [34] found that the flame intermittently lifts off from its anchoring surface due the acoustic perturbations. In the lift-off state, the flame dynamics is significantly influenced by the underlying hydrodynamic fluctuations of the unburnt reactants. When the timescales of these flow fluctuations are much larger than the reaction timescales in the system [35], the flame ceases to exist in the system and is blown out. After flame blowout, the amplitude of the pressure fluctuations reduces to a very small value. Flame blowout can lead to unplanned shutdowns of power plants, sudden loss of thrust in airplane engines, etc. [36].

We come across a mathematical model such as coupled logistic maps with quasi-periodic forcing that closely represent the dynamics of the thermoacoustic system observed in experiments. Depending on the range of operating parameters, this model shows a transition from a state of synchronized quasi-periodic motion to nonsynchronized chaotic motion (intermittency) via blowout bifurcation [37–39]. During blowout bifurcation, the synchronized behavior loses its transverse stability and attains desynchronized behavior [37,38]. The repelled trajectory from the unstable synchronization manifold either moves to a new stable attractor or moves to infinity [38]. If the trajectory reaches to a new attractor, then the system displays desynchronized behavior. In contrast, if the trajectory moves to infinity, then we call this state as attractor blowout. We can associate this repulsive behavior of a manifold to a catastrophic event. In the present study, we investigate the dynamical behavior of extreme events observed prior to such catastrophic transition in the model of coupled logistic maps with quasi-periodic forcing. Thus, in both the thermoacoustic system and the model of coupled logistic maps with quasi-periodic forcing, flame blowout and attractor blowout, respectively, can be considered as catastrophic transitions. There is potential scientific importance in identifying the existence of such critical transitions and obtain early warning signals for their onset.

In our analysis, we choose the parameter range of both the systems such that their behavior shows regular oscillations (*e.g.*, quasi-periodicity), intermittency, and extreme events leading to a catastrophic transition. The dynamics of extreme events exhibits the occurrence of both large- and small-amplitude events in the system. The distribution of such events follows a power law [26]. Further, we observe that, just prior to the catastrophic transition, extreme events display a special kind of distribution that deviates from the power law, known as the dragon-king distribution. Therefore, we propose for the first time that the existence of such dragon-king extreme events can be a precursor for catastrophic transitions. To the best of our knowledge, no such early warning signal for catastrophic transitions has been reported before. We confirm the existence of dragon-king events using a probability distribution function, a complementary cumulative distribution function (CCDF), and finding p-values of a dragon-king test (DK-test) [22,23].

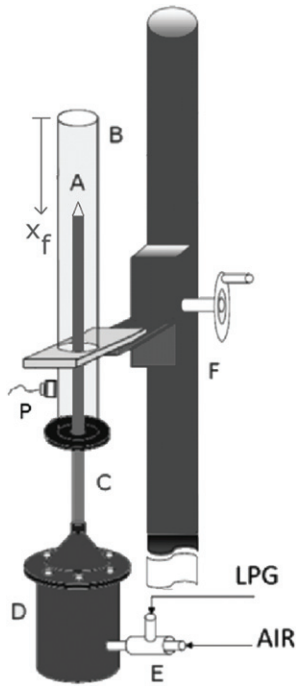

Fig. 1: Schematic of the experimental facility of a thermoacoustic system. A: a single conical flame. B: an open-closed glass duct. C: a burner tube. D: a decoupler. E: an LPG-air premixing chamber. F: a traverse. P: a pressure sensor. The figure is reproduced with permission from Kabiraj and Sujith [34].

Catastrophic transition in a thermoacoustic system. – The experiments were performed on a ducted premixed laminar flame combustor (fig. 1). The details of the setup and operating parameters can be found from Kabiraj and Sujith [34]. Here, we briefly mention the relevant information of the system and the data acquisition required for our analysis. The combustor is made up of a vertical glass duct closed at the bottom and open at the top. A burner tube is used to supply a premixed mixture of air and fuel (liquefied petroleum gas (LPG)) required for combustion. A single conical flame was stabilized at the tip of the burner tube. During experiments, the location of the flame with respect to the open end of the glass duct was varied as the control parameter and is denoted as x_f. Towards this purpose, the duct is moved vertically with respect to the burner tube using a traverse arrangement, while the absolute position of the burner tube is held fixed throughout the experiments. The acoustic pressure fluctuations in the system, corresponding to each flame location, were measured using a piezoelectric pressure transducer

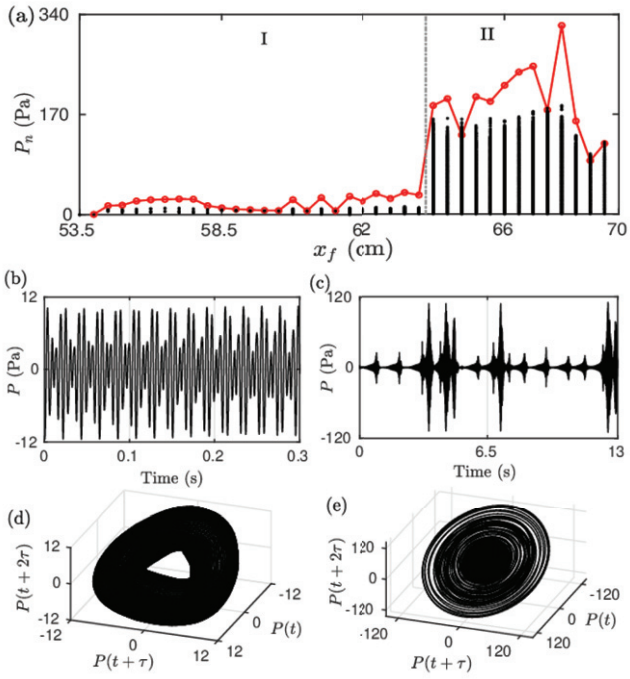

Fig. 2: One-parameter bifurcation diagram shows the variation of the local maxima P_n of the absolute values of acoustic pressure fluctuations ($|P|$) as a function of the flame location (x_f), obtained from experiments performed on a thermoacoustic system. A red line connecting open circles shows a limiting value of the critical threshold calculated from eq. (1) for identifying extreme events. Region I corresponds to regular oscillations (*i.e.*, limit cycle and quasi-periodicity) and region II indicates bursting oscillations (*i.e.*, intermittency and extreme events). ((b), (c)) Time series and ((d), (e)) the reconstructed phase portraits of quasi-periodicity ($x_f = 61$ cm, embedding dimension $d = 7$ and time delay $\tau = 1.5$ ms) and intermittency ($x_f = 68$ cm, $d = 7$ and $\tau = 1.9$ ms), respectively.

(PCB piezotronics, Model Number 103B02, uncertainty 0.14 Pa). The data were acquired for 30 s at a sampling frequency of 10 kHz.

Kabiraj and Sujith [34] showed that, as the flame location was varied in this system, the dynamic behavior changes from the state of fixed point, limit cycle, quasi-periodicity, and intermittency to flame blowout. In the present investigation, we aim to provide a precursor for a catastrophic transition, *i.e.*, flame blowout, observed in this system.

We first present the dynamical transitions observed in the thermoacoustic system as a one-parameter bifurcation diagram in fig. 2(a). The bifurcation diagram is drawn in the form of the distribution of all local maxima (P_n) observed in the time series of the absolute value of pressure ($|P|$) as a function of the flame location (x_f). Since each local maxima P_n represents the absolute amplitude of a signal, we refer to P_n as an event. In region I (53.5 cm $\leq x_f <$ 64 cm) of fig. 2(a), we observe the states of low-amplitude limit cycle oscillations (53.5 cm $< x_f <$ 61 cm) and quasi-periodic oscillations (61.5 cm $< x_f <$ 64 cm). During these regular dynamical states, the deviation of the pressure amplitudes from their mean value is less. In region II of fig. 2(a) (64 cm $\leq x_f <$ 70 cm), we observe the scatter of local amplitudes in the signal over a larger range due to the state of intermittency.

To delineate quasi-periodicity ($x_f = 61$ cm) and intermittency ($x_f = 68$ cm) behaviors, we plot their time series in figs. 2(b), (c). The corresponding phase portraits are reconstructed via delay coordinate embedding [40] and are shown in figs. 2(d), (e), respectively. The phase space trajectory of a quasi-periodic signal exhibits a bounded motion around a torus attractor (fig. 2(d)). During intermittency (fig. 2(c)), the pressure oscillations alternately switch between epochs of low-amplitude periodic oscillations and bursts of large-amplitude chaotic oscillations [34]. The phase space corresponding to this state shows a disk-like attractor (fig. 2(e)), where the trajectory spirals towards the outer core during the occurrence of burst and gets re-injected back to the center core at the end of it. Kabiraj and Sujith [34,41] characterized this state of intermittency as type-II intermittency using the return map and recurrence plot analysis. Furthermore, at flame locations beyond $x_f >$ 70 cm, the system experiences a catastrophic transition, *i.e.*, flame blowout.

In region II, at a few flame locations, we observe the state of extreme events in the acoustic pressure oscillations. To identify such extreme events, we consider a critical amplitude threshold (P_n^{EE}) that can be calculated using the following equation [42]:

$$P_n^{EE} = \langle P_n \rangle + N\sigma_{P_n}, \tag{1}$$

where the mean and standard deviation of all P_n in the signal are denoted by $\langle P_n \rangle$ and σ_{P_n}, respectively. For an event to be considered an extreme event, it must satisfy the condition $P_n^{EE} < P_n$ [42]. The multiplication factor N can be considered as $N \geq 4$ [43–45] for finding the critical threshold. The value of N is selected from several trials. A low value of N can cause the occurrence of many events inside the threshold, while a high value of N can lead to the identification of a few events in the signal. As mentioned before, since the occurrence of extreme events is rare, we need to choose an optimum value of N to have only a few events that cross the threshold in a signal. Based on eq. (1), we identify extreme events in the experimental data by fixing $N = 8$ (see figs. 3(a), (b)). We indicate this critical threshold at each x_f by a line connecting red circles over the one-parameter bifurcation diagram in fig. 2(a). For a given x_f, if an event in $|P|$ crosses the threshold line, we consider the corresponding event to be an extreme event. In regime II of intermittency, we notice that at a few values of x_f, such as $x_f = 64.5$, 66.5, 69, and 69.5 cm, the pressure amplitude (P_n) crosses the critical amplitude threshold (P_n^{EE}). Therefore, we consider such events as extreme events in our analysis.

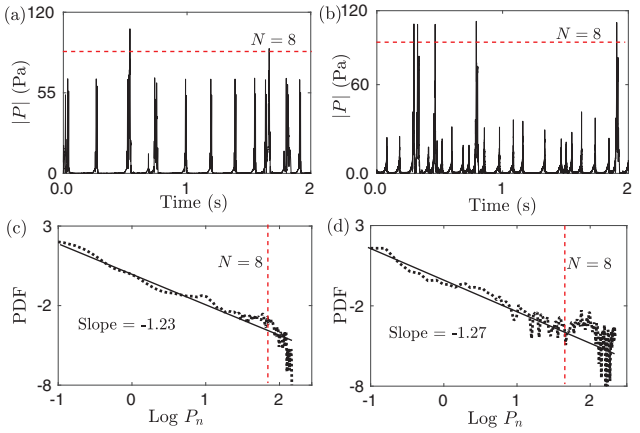

Fig. 3: (a), (b): absolute values of pressure fluctuations corresponding to two distinct extreme events for $x_f = 69\,\text{cm}$ and $x_f = 69.5\,\text{cm}$, respectively. (c), (d): the corresponding probability distribution functions (PDFs) of P_n on a log-log scale. In the calculation of PDF, we use the entire recorded pressure signal. A red dashed line in (a)–(d) shows the threshold value corresponding to $\langle P_n \rangle + 8\sigma_{P_n}$. The straight line fits (solid line) for the linear regime of the PDFs and the corresponding slopes are shown in (c) and (d).

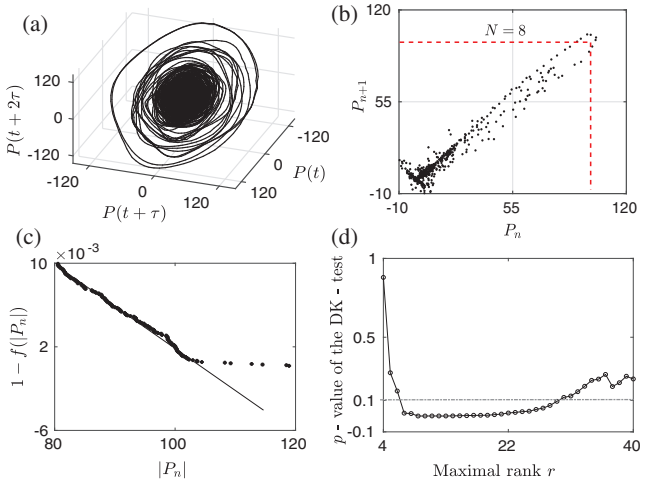

Fig. 4: (a) The reconstructed phase portrait (using embedding dimension $d = 7$ and time delay $\tau = 1.9\,\text{ms}$); (b) Poincaré return map; (c) complementary cumulative distribution function (CCDF); and (d) the variation of p-values of the DK test as a function of the maximal rank r corresponding to the pressure signal observed during dragon-king extreme events at $x_f = 69.5\,\text{cm}$.

In figs. 3(a) and (c), we show time series (in terms of the absolute value of pressure amplitude, $|P|$) corresponding to the states of extreme events observed at two flame locations ($x_f = 69\,\text{cm}$ and $x_f = 69.5\,\text{cm}$, respectively) in the system. The probability distribution function (PDF) of the local maxima in the signals corresponding to these states are illustrated in figs. 3(c) and (d). A red dashed line in figs. 3(a) to (d) represents the critical threshold based on eq. (1) used for defining extreme events in the system. Interestingly, we notice that these two extreme events have different PDFs. The extreme events shown in fig. 3(c) have a distribution that, in turn, indicates that all the events in the signal can be well fitted with a power law. However, the PDF shown in fig. 3(d) exhibits a distinct hump-like long-tail distribution (dragon-king–like distribution), where we observe that a few events at the tail deviate from the power-law distribution of the rest of the events. This kind of distribution is known as a dragon king [22,23]. Interestingly, we notice that the dragon-king extreme events appear only just prior to flame blowout. Hence, we propose that the identification of dragon-king extreme events in the pressure signal can serve as a precursor for a catastrophic transition, such as flame blowout, in thermoacoustic systems.

Further, to understand the characteristics of dragon-king extreme events, we show the reconstructed phase portrait and the Poincaré return map of the acoustic pressure signal (shown in fig. 3(b)) in figs. 4(a) and (b), respectively. In fig. 4(a), we notice that the trajectory stays within the inner core region corresponding to the low-amplitude cluttered behavior for most of the time interval. Then, the trajectory is pushed away from the inner core region during the onset of large-amplitude events [34]. Since the system has a single attractor in the inner core, the trajectory returns to it after a few revolutions, at the end of the large-amplitude events. Furthermore, we show the Poincaré return map in fig. 4(b), obtained by plotting the first local maxima (P_n) against the next local maxima (P_{n+1}). We notice that some events cross the critical threshold (represented by a dashed line in fig. 4(b)), which confirms the existence of extreme events.

Next, we confirm the presence of dragon-king extreme events using the measure of complementary cumulative distribution function (CCDF), $(1 - f(x))$ [23], where x is the given signal. The mathematical details of CCDF are provided in sect. II of the Supplementary Material `Supplementarymaterial.pdf` (SM). In fig. 4(c), black points indicate the CCDF obtained from the pressure signal and the solid black line denotes the corresponding power-law fit. We observe that in the tail of the CCDF, there are events outside the power-law fit. These events are outliers from the power-law distributions, which indicate the nature of dragon kings [23]. However, in the case of quasi-periodic oscillations (fig. 2(b)) and extreme events (fig. 3(a)), we do not observe such outliers (see figs. 1(a), (c) in sect. II of the SM).

Further, to corroborate the existence of dragon kings, we find the p-value of DK test [23]. The p-value of the DK test helps us to identify whether the null hypothesis is true or false. If the null hypothesis is true, then the given data set has no DK extreme events or vice versa. A smaller p-value indicates that some of the events in the given data set have a different distribution than the power-law distribution; thus, the null hypothesis fails. In contrast, a larger

p-value indicates that the null hypothesis is satisfied. The p-values are obtained using the following relation:

$$p = 1 - F(T_s, 2r, 2(n-r)), \tag{2}$$

where T_s, r and n are the test statistic, rank of the events, and number of the events, respectively. $F(T_s, 2r, 2(n-r))$ is the cumulative distribution function of the f-distribution with $(2r, 2(n-r))$ degrees of freedom. The mathematical details for obtaining the p-value from DK test are provided in sect. I of the SM. A lower p-value obtained from the DK test signifies that the null hypothesis of the generation of all events in a signal by the same distribution (*i.e.*, having the power-law distribution) is not valid. In the literature of extreme events [22,23], if the p-value is less than 0.1, the existence of dragon kings in a signal is confirmed. In fig. 4(d), we found that p-values for the pressure signal corresponding to $x_f = 69.5\,\text{cm}$ are less than 0.1. Therefore, using the DK test we confirm the presence of dragon-king extreme events prior to the catastrophic transition observed in the thermoacoustic system.

Catastrophic transition in a coupled logistic maps with quasi-periodic forcing. – As we discussed in the introduction, catastrophic transitions appear in other nonlinear dynamical systems as well. In order to show the generality of the existence of dragon kings before catastrophic transitions, we consider a system of coupled logistic maps with quasi-periodic forcing that exhibits a catastrophic transition [38],

$$\begin{aligned} x_{n+1} &= \alpha x_n(1-x_n) + \beta(y_n - x_n) + \eta\cos(2\pi\theta_n), \\ y_{n+1} &= \alpha y_n(1-y_n) + \beta(x_n - y_n) + \eta\cos(2\pi\theta_n), \\ \theta_{n+1} &= \theta_n + \omega, \end{aligned} \tag{3}$$

where x, y, θ are the system variables, α and β are the strengths of nonlinearity and the strength of coupling, respectively. η and ω are the amplitude and the frequency of the external driving force, respectively.

The model in eq. (3) exhibits the transition from the state of quasi-periodicity to intermittency and then to attractor blowout (as shown in fig. 6). Here, attractor blowout is a catastrophic transition wherein the attractor disappears (*i.e.*, moves to infinity) due to a change in the control parameter. In fig. 5(a), we plot the absolute values of synchronization error, *i.e.*, $|x_n - y_n|$, as a function of the parameter α for a fixed value of parameters, $\beta = 0.156$, $\omega = (\sqrt{5}-1)/2$ and $\eta = 0.01$. Here, the black dotted points correspond to $|x_n - y_n|$ and a red line connected by open red circles denotes the boundary of the critical threshold obtained for $N = 6$ [43,44].

For lower values of α in fig. 5(a), we observe synchronization of the variables x and y, causing the synchronization error to remain near zero. However, for higher values of α, we notice large fluctuations in the synchronization error, which happen due to the desynchronization of x and y variables.

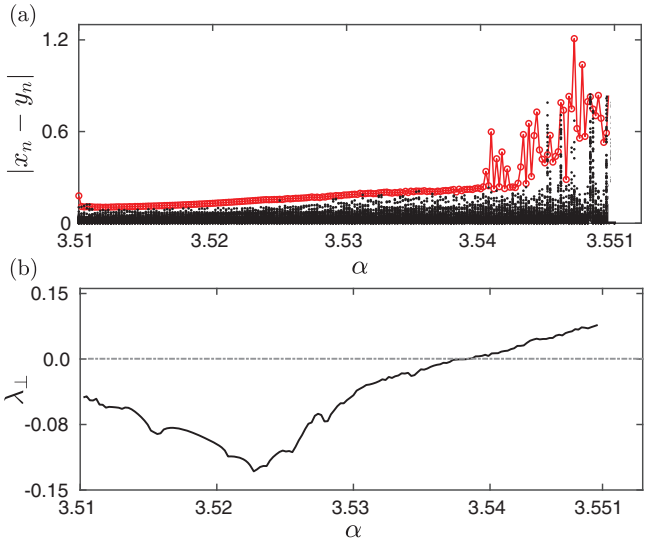

Fig. 5: One parameter bifurcation diagram for a system of coupled logistic maps with quasi-periodic forcing, showing the variation of (a) synchronization error and (b) transverse Lyapunov exponent as a function of α. We fix the other system parameters as $\beta = 0.156$, $\omega = (\sqrt{5}-1)/2$ and $\eta = 0.01$.

Further, we calculate the transverse Lyapunov exponent (TLE) to identify the transition from synchronized to desynchronized states. The expression for the transverse Lyapunov exponent for eq. (3) can be obtained as [38]

$$\lambda_\perp = \lim_{N\to\infty} \frac{1}{N} \sum_{n=1}^{N} \ln|f'_\alpha(x_n) - 2\beta|. \tag{4}$$

The function corresponding to variable x is defined as $f_\alpha(x) = \alpha x(1-x)$ and its derivative is denoted by f'_α. We choose the system parameter as $\beta = 0.156$. The definition of TLE is elaborated in sect. III of the SM. The synchronized regime is confirmed through the negative values of the TLE ($\lambda_\perp$) [38], as seen in fig. 5(b). However, for increasing the α value, we notice that the synchronized attractor loses its transverse stability, leading to desynchronized behavior through blowout bifurcation (occurs when $\lambda_\perp$ crosses zero). When the TLE becomes positive, the synchronized invariant manifold turns out to be a repeller. Hence, the trajectory is repelled from the synchronization manifold and it moves to another attractor in the phase space and shows the behavior of on-off intermittency [38]. Such intermittency dynamics exists for a range of system parameters $\alpha \in (3.54, 3.552)$.

Furthermore, we notice some states of intermittency that satisfy the criteria for extreme events as given in eq. (1). Extreme events can be identified from a few intermittency events that cross the boundary of the critical threshold (fig. 5(a)). Such a behavior of the presence of extreme events in the region of intermittency shows a qualitative match with that observed in the thermoacoustic system (fig. 2(a)). Upon increasing α, the attractor

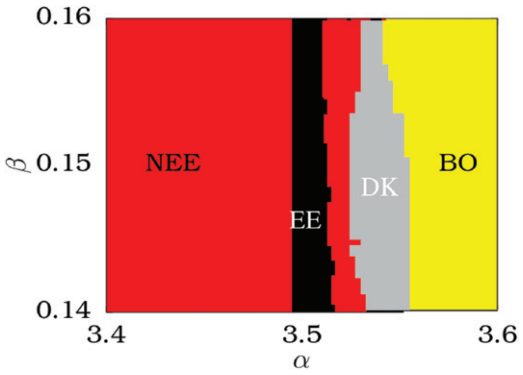

Fig. 6: A two-parameter bifurcation diagram between α and β for a system of coupled logistic maps with quasi-periodic forcing. NEE (in red) and EE (in black) denote the regions of nonextreme events and extreme events, respectively. DK (in grey) and BO (in yellow) indicate the regions of dragon-king extreme event and attractor blowout, respectively.

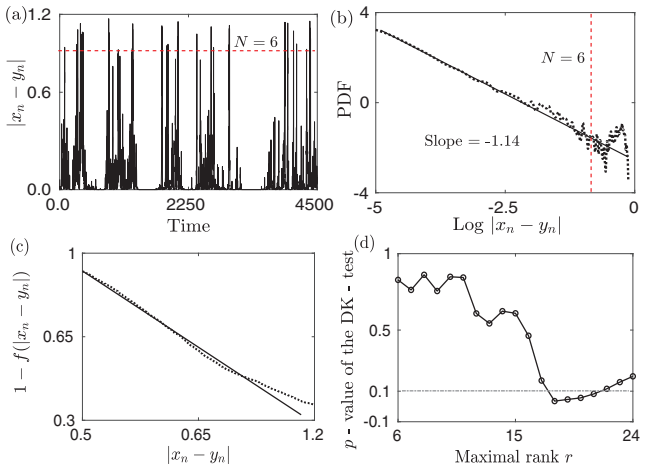

Fig. 7: (a) Time evolution and (b) probability distribution function (in log-log scale) of dragon-king extreme events in a model; (c) complementary cumulative distribution function; and (d) the variation of p-value of the DK-test as a function of the maximal rank r of the signal corresponding to the dragon-king extreme events. We fix the other system parameters as $\alpha = 3.55$, $\beta = 0.156$, $\omega = (\sqrt{5}-1)/2$ and $\eta = 0.01$.

diverges to infinity. This means that the repelled attractor from the unstable synchronization manifold does not reach any attractor state in the phase space. We characterize this transition to a state with the absence of attractors as a catastrophic transition.

Next, we illustrate the dynamical transition of this model in a two-dimensional parameter space between α and β. We separate the dynamical regimes in fig. 6 collectively using different measures, *i.e.*, the transverse Lyapunov exponent, the extreme event criterion, and the DK test. We identify four different dynamical regimes in the model, including i) no extreme events (NEE, marked in red containing quasi-periodic and intermittency dynamics with no extreme events); ii) extreme events (EE, marked in black containing intermittency and extreme events); iii) dragon-king extreme events (DK, marked in gray containing extreme events with dragon-king distribution); and iv) attractor blowout regime (marked in yellow). In fig. 6, we notice the presence of a regime of dragon-king extreme events prior to attractor blowout. Therefore, we suggest that the dragon kings can be a precursor for the catastrophic transition in the model as well. Next, we confirm the existence of dragon-king extreme events through a statistical analysis.

In figs. 7(a) and (b), we show the time variation of $|x_n - y_n|$ and the corresponding PDF, respectively, for the state of dragon-king extreme event. We notice the existence of hump-like behavior at the tail of the distribution in fig. 7(b). This long-tail distribution with a hump confirms the existence of dragon kings in the system [22,23].

Further, to confirm the presence of dragon-king events, we also plot complementary cumulative distribution function (CCDF) in fig. 7(c) corresponding to the time series shown in fig. 7(a). We notice that the tail of the CCDF (shown as a dotted black line) deviates from the rest of the power-law distribution (indicated by a black solid line). Further, the CCDF corresponding to the quasi-periodic attractor and extreme events follows a power-law distribution (refer to figs. 1(b), (d) in sect. II of the SM). Furthermore, we plot the variation of p-values as a function of the maximal rank r in fig. 7(d). We notice that initially p-value has a value greater than 0.1 and less than 0.9. However, after a certain range of maximal rank, it takes a value less than 0.1, confirming the existence of dragon kings in the coupled logistic maps with quasi-periodic forcing, before the onset of attractor blowout [22,23].

Conclusion. – To summarize, we found the existence of dragon-king extreme events prior to a catastrophic transition in the experimental study performed on a thermoacoustic system and in a model of coupled logistic maps with quasi-periodic forcing. The existence of dragon kings is confirmed using several measures, such as probability distribution function, complementary cumulative distribution function, and the DK test. We propose that the presence of dragon kings can serve as an early warning signal to catastrophic transitions observed in these systems. We believe that the present study opens a new direction for understanding the mechanism of catastrophic transitions in nonlinear dynamical systems.

* * *

DP, SAP and RIS gratefully acknowledge the Office of Naval Research Global (ONRG) USA (N62909-18-1-2061, Contract Monitor: Dr. R. Kolar) and J. C. Bose fellowship (JCB/2018/000034/SSC) from Department of Science and Technology (DST) India, MHRD and IIT Madras (SB/2021/0845/AE/MHRD/002696) for the financial support. KS is supported by the UGC, Government of India through Dr. D. S. Kothari Postdoctoral

Fellowship. AP acknowledges "loE, University of Delhi as FRP grant" (loE/FRP/PCMS/2020/27) for financial support.

REFERENCES

[1] Albeverio S., Jentsch V. and Kantz H., *Extreme Events in Nature and Society, The Frontiers Collection* (Springer, Berlin) 2006.

[2] Sornette D., *Critical Phenomena in Natural Sciences: Chaos, Fractals, Self-Organization and Disorder: Concepts and Tools* (Springer, New York) 2006.

[3] Nicolis G. and Nicolis C., *Foundations of Complex Systems*, 2nd edition (World Scientific, Singapore) 2012.

[4] Montroll E. W. and Badger W. W., *Introduction to Quantitative Aspects of Social Phenomena* (Gordon and Breach, New York) 1974.

[5] Höhmann R., Kuhl U., Stöckmann H. J., Kaplan L. and Heller E. J., *Phys. Rev. Lett.*, **104** (2010) 093901.

[6] Metzger J. J., Fleischmann R. and Geisel T., *Phys. Rev. Lett.*, **112** (2014) 203903.

[7] Mathis A., Froehly L., Toenger S., Dias F., Genty G. and Dudley J. M., *Sci. Rep.*, **5** (2015) 12822.

[8] Birkholz S., Brée C., Veselić I., Demircan A. and Steinmeyer G., *Sci. Rep.*, **6** (2016) 35207.

[9] Kharif C. and Pelinovsky E., *Eur. J. Mech. B*, **22** (2003) 603.

[10] Shukla P. K., Kourakis I., Eliasson B., Marklund M. and Stenflo L., *Phys. Rev. Lett.*, **97** (2006) 094501.

[11] Baronio F., Conforti M., Degasperis A., Lombardo S., Onorato M. and Wabnitz S., *Phys. Rev. Lett.*, **113** (2014) 034101.

[12] Kibler B., Chabchoub A., Gelash A., Akhmediev N. and Zakharov V. E., *Phys. Rev. X*, **5** (2015) 041026.

[13] Onorato M., Waseda T., Toffoli A., Cavaleri L., Gramstad O., Janssen P. A. E. M., Kinoshita T., Monbaliu J., Mori, Osborne A. R., Serio M., Stansberg C., Tamura H. and Trulsen K., *Phys. Rev. Lett.*, **102** (2009) 114502.

[14] Solli D. R., Ropers C., Koonath P. and Jalali B., *Nature*, **450** (2007) 1054.

[15] Ganshin A. N., Efimov V. B., Kolmakov G. V., Mezhov-Deglin L. P. and McClintock P. V. E., *Phys. Rev. Lett.*, **101** (2008) 065303.

[16] Bailung H., Sharma S. K. and Nakamura Y., *Phys. Rev. Lett.*, **107** (2011) 255005.

[17] Pisarchik A. N., Jaimes-Reátegui R., Sevilla-Escoboza R., Huerta-Cuellar G. and Taki M., *Phys. Rev. Lett.*, **107** (2011) 274101.

[18] Bonatto C., Feyereisen M., Barland S., Giudici M., Masoller C., Ríos Leite J. and Tredicce J., *Phys. Rev. Lett.*, **107** (2011) 053901.

[19] Kovalsky M. G., Hnilo A. A. and Tredicce J. R., *Opt. Lett.*, **36** (2011) 4449.

[20] Zamora-Munt J., Garbin B., Barland S., Giudici M., Rios Leite J. R., Masoller C. and Tredicce J. R., *Phys. Rev. A*, **87** (2013) 035802.

[21] Karnatak R., Ansmann G., Feudel U. and Lehnertz K., *Phys. Rev. E*, **90** (2014) 022917.

[22] Sornette D., *Int. J. Terraspace Sci. Eng.*, **1** (2009) 1.

[23] Pisarenko V. F. and Sornette D., *Eur. Phys. J. ST*, **205** (2012) 95.

[24] Mishra A., Leo Kingston S., Hens C., Kapitaniak T., Feudel U. and Dana S. K., *Chaos*, **30** (2020) 063114.

[25] Saha A. and Feudel U., *Phys. Rev. E*, **95** (2017) 062219.

[26] De S. Cavalcante H. L. D., Oriá M., Sornette D., Ott E. and Gauthier D. J., *Phys. Rev. Lett.*, **111** (2013) 198701.

[27] Mishra A., Saha S., Vigneshwaran M., Pal P., Kapitaniak T. and Dana S. K., *Phys. Rev. E*, **97** (2018) 062311.

[28] Sornette D. and Ouillon G., *Eur. Phys. J. ST*, **205** (2012) 1.

[29] Lieuwen T. C. and Yang V., *Combustion Instabilities in Gas Turbine Engines: Operational Experience, Fundamental Mechanisms, and Modeling* (American Institute of Aeronautics and Astronautics) 2005.

[30] Kabiraj L., Saurabh A., Wahi P. and Sujith R. I., *Chaos*, **22** (2012) 023129.

[31] Kashinath K., Waugh I. C. and Juniper M. J., *Fluid Mech.*, **761** (2014) 399.

[32] Juniper M. P. and Sujith R. I., *Annu. Rev. Fluid Mech.*, **50** (2018) 661.

[33] Premraj D., Pawar S. A., Kabiraj L. and Sujith R. I., *EPL*, **128** (2020) 54005.

[34] Kabiraj L. and Sujith R. I., *J. Fluid Mech.*, **713** (2012) 376.

[35] Law K. C., *Combustion Physics* (Cambridge University Press) 2010.

[36] Shanbhogue S. J., Husain S. and Lieuwen T., *Prog. Energy Combust. Sci.*, **35** (2009) 98.

[37] Ott E. and Sommerer J. C., *Phys. Lett. A*, **188** (1994) 39.

[38] Neumann E., Sushko I., Maistrenko Y. and Feudel U., *Phys. Rev. E*, **67** (2003) 026202.

[39] Weng Y., Unni V. R., Sujith R. I. and Saha A., *Nonlinear Dyn.*, **100** (2020) 3295.

[40] Kantz H. and Schreiber T., *Nonlinear Time Series Analysis* (Cambridge University Press) 2004.

[41] Kabiraj L., Sujith R. I. and Wahi P., *Fluid Dyn. Res.*, **44** (2012) 031408.

[42] Dysthe K., Krogstad H. E. and Müller P., *Annu. Rev. Fluid Mech.*, **40** (2008) 287.

[43] Bonatto C. and Endler A., *Phys. Rev. E*, **96** (2017) 012216.

[44] Reinoso J. A., Jordi Z. M. and Masoller C., *Phys. Rev. E*, **87** (2013) 062913.

[45] Suresh K. and Pisarchik A. N., *Phys. Rev. E*, **98** (2018) 032203.